

Supplemental Material: Unravelling the origin of capacity fade in Prussian white hard carbon full cells through *operando* X-ray diffraction

Ida Nielsen,^{1,*} Charles Aram Hall,¹ Agnes-Matilda Mattsson,¹ Reza
Younesi,¹ Alexander Buckel,² Gustav Ek,¹ and William R. Brant^{1,†}

¹*Department of Chemistry - Ångström Laboratory,
Uppsala University, Box 538, SE-751 21 Uppsala, Sweden.*

²*Altris AB, Kungsgatan 70b, SE-753 18 Uppsala, Sweden*

* Corresponding author ida.nielsen@kemi.uu.se

† Corresponding author william.brant@kemi.uu.se

Effect of the electrolyte

In this study, two different electrolyte systems were used: NaPF_6 in EC:DEC (S cells) and NaBOB in TEP (BOB cells). The cells S4/BOB3 and S6/BOB6 were pre-cycled using similar potential ranges but with different electrolyte systems. Even though it is hard to compare the two electrolyte systems due to their different natures and the higher number of pre-cycles for the BOB cells, they seem to behave similarly with similar amounts of the $\text{Fm}\bar{3}\text{m}$ phase fraction and capacity at the end of discharge. However, cell S6 has a lower discharge capacity relative to cell BOB6 which might be due to the disrupted cycling behavior at the very beginning of the beamtime cycling (grey curve in Figure S3) leading to a restart of the cell. Nevertheless, the impact of the electrolyte is negligible and both electrolyte systems can be used for long-term cycling of PW-based batteries.

Figures and tables

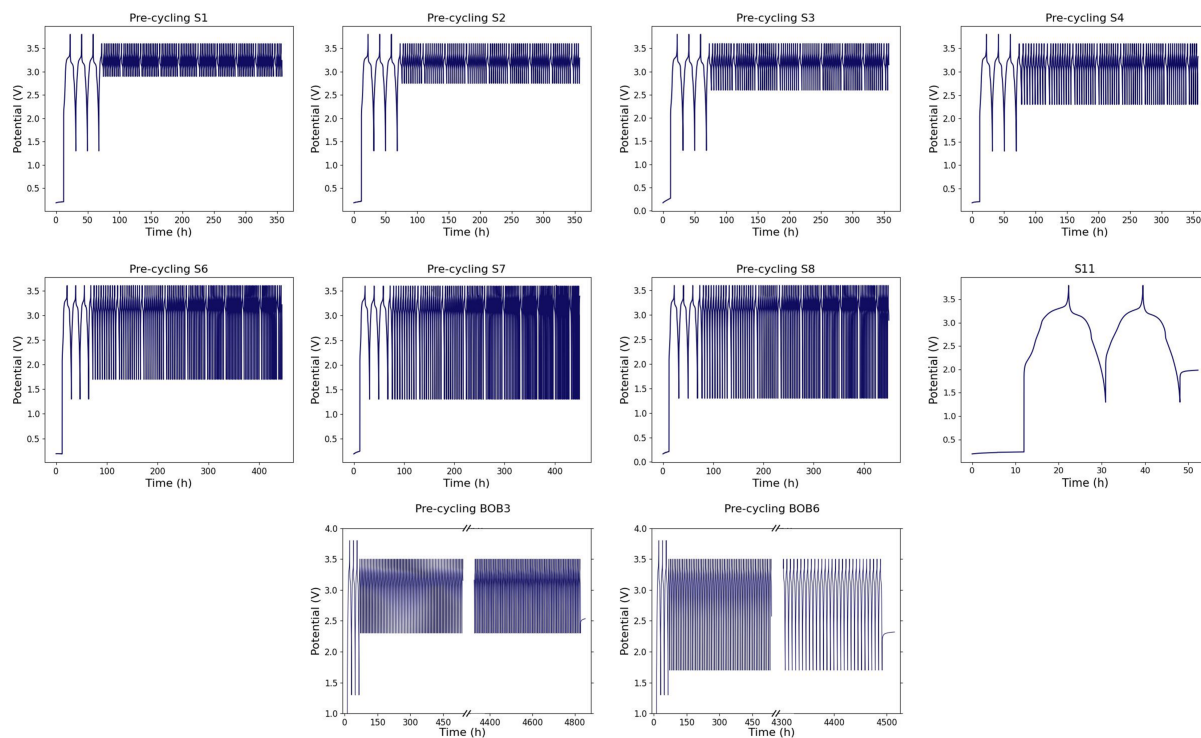


Figure S1. Pre-cycling data for all cells. The pre-cycling conditions are specified in Table S1 below.

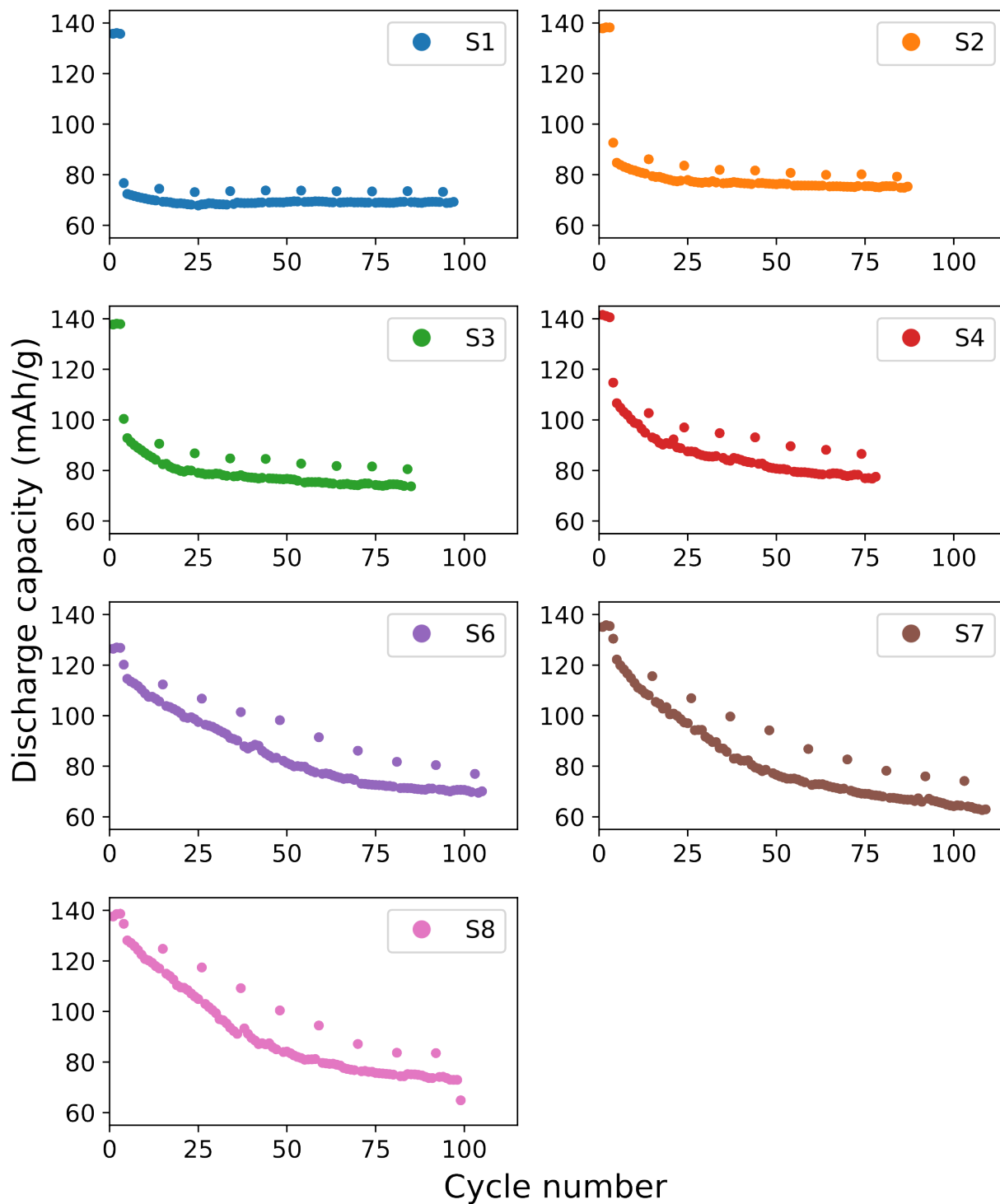


Figure S2. Long-term cycling data for all cells. The pre-cycling conditions are specified in Table S1 below.

Table S1. Overview of all cells included in this study including the cell name, the number of formation and pre-cycles, pre-cycling range, and the beamtime cycling.

Cell name	Formation cycles	Pre-cycles	Pre-cycle range	Beamtime cycling
S1	3	94	2.9-3.6 V	1.3-3.6 V, 2·C/5
S2	3	84	2.75-3.6 V	1.3-3.6 V, 2·C/5
S3	3	82	2.6-3.6 V	1.3-3.6 V, 2·C/5
S4	3	75	2.3-3.6 V	1.3-3.6 V, 2·C/5
S6	3	102	1.7-3.6 V	1.3-3.6 V, 2·C/5
S7	3	106	1.3-3.6 V	1.3-3.6 V, 2·C/5
S8	3	96	1.3-3.6 V	1.3-3.6 V, 1·C/10 + 1·C/3
S10	0	0		1.3-3.6 V, 2·C/5
S11	2	0	1.3-3.8 V	1.3-3.6 V, 2·C/5
BOB3	3	730	2.3-3.5 V	1.3-3.5 V, 2·C/5
BOB6	3	605	1.7-3.5 V	1.3-3.5 V, 2·C/5
BOB7	0	0		1.3-3.5 V, 2·C/5

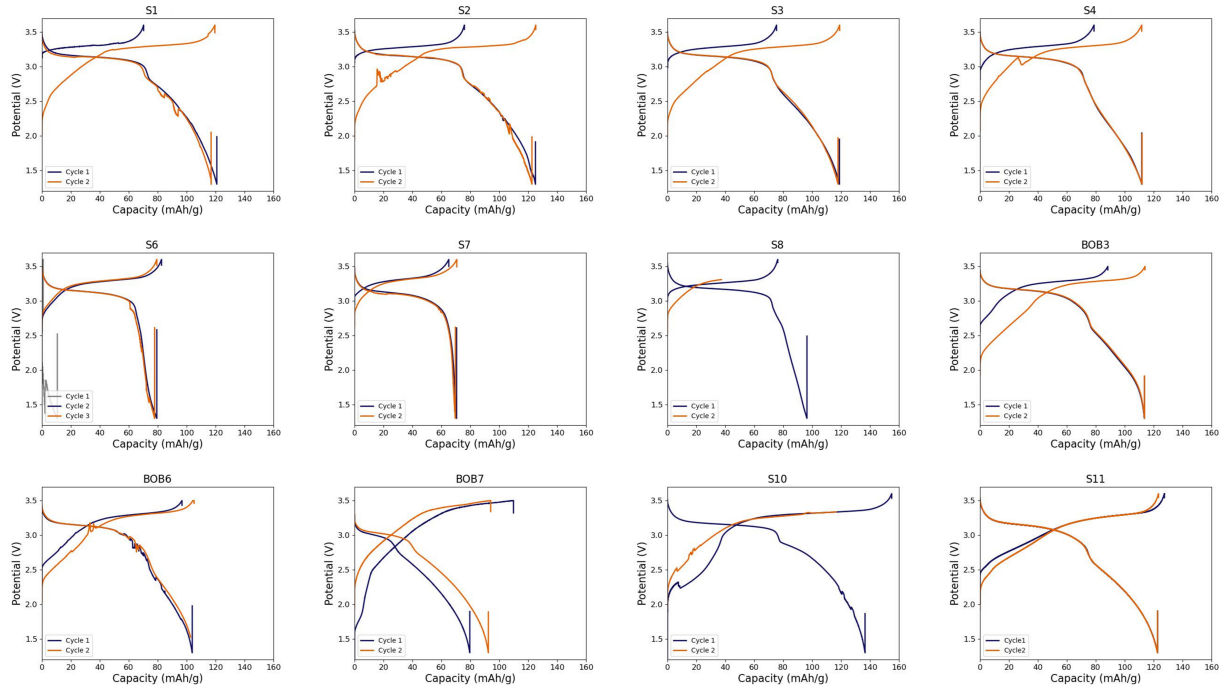


Figure S3. Beamtime cycling data for all cells. All cells were cycled in the potential range of 1.3 to 3.6 V (to 3.5 V for the BOB cells) with a current of $C/5$ except for cell S8 which was cycled using a current of $C/10$.

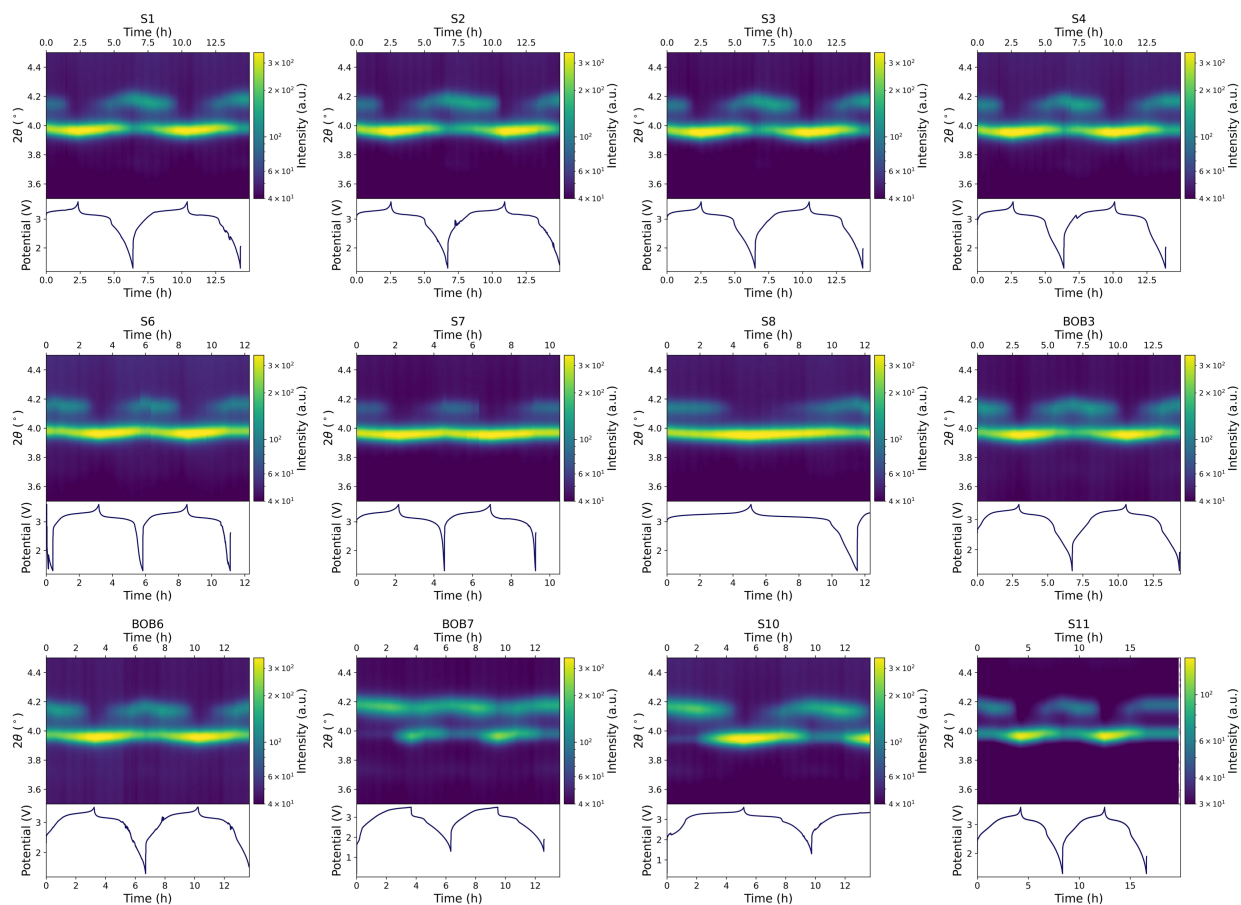


Figure S4. Contour maps of the SXR D data for all cells with the corresponding electrochemical cycling. All cells were cycled in the potential range of 1.3 to 3.6 V (to 3.5 V for the BOB cells) with a current of $C/5$ except for cell S8 which was cycled using a current of $C/10$.

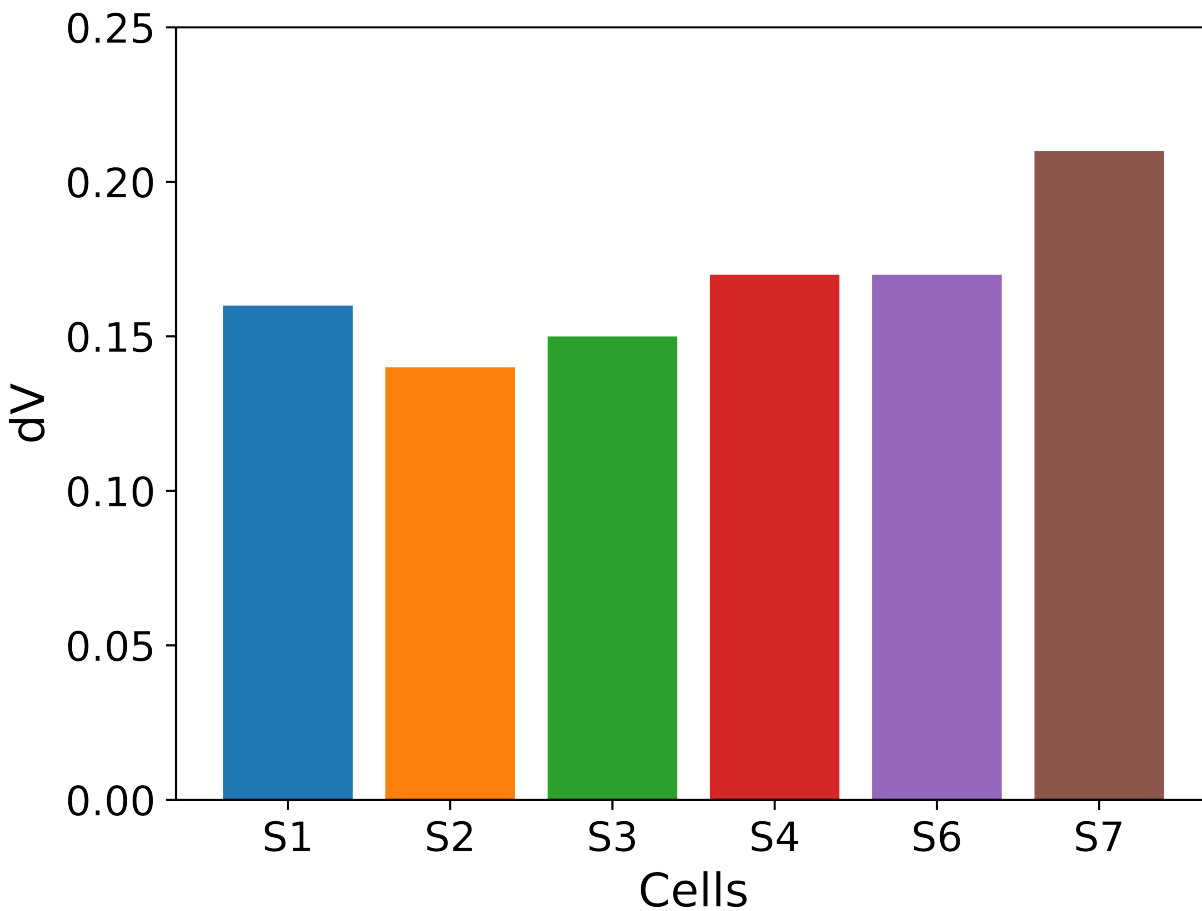


Figure S5. Estimated overpotentials for cells S1 to S7 calculated by taking the voltage difference between the lower and upper voltage plateau for the first discharge and second charge of the beamtime cycling.^a

^a A. Buckel *et al.* Batter. Supercaps, 2023, 202300533

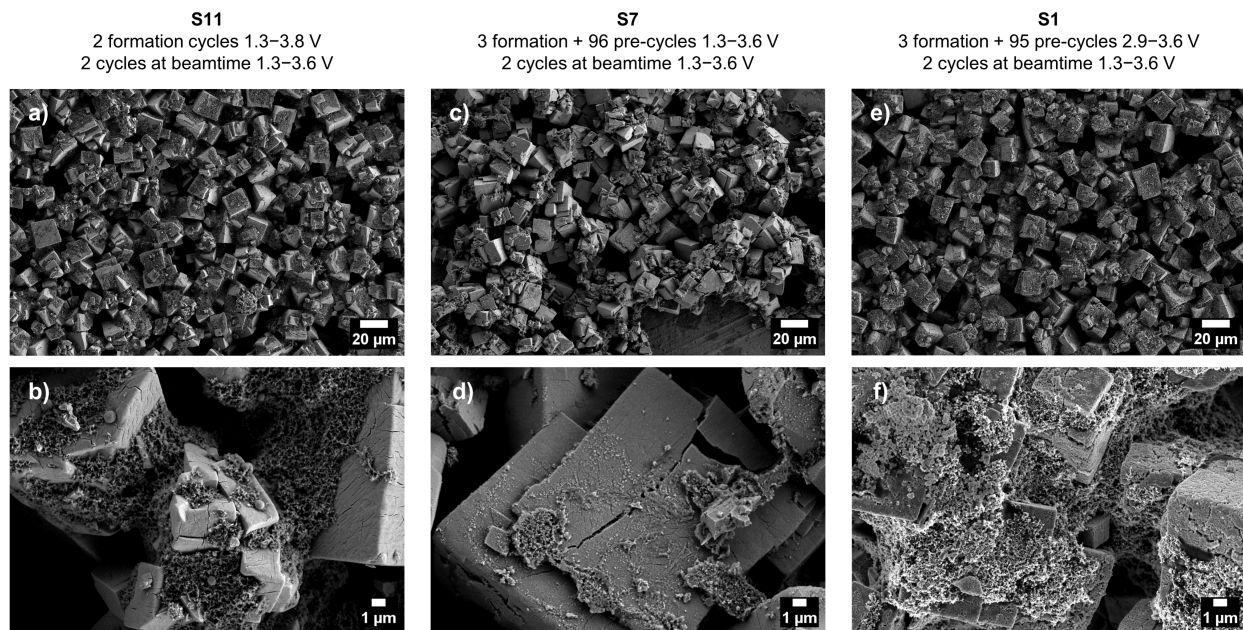


Figure S6. SEM images of the cells a-b) S11, c-d) S7, and e-f) S1. The images were obtained using an accelerating voltage of 3 kV and a working distance of 6.7 mm.

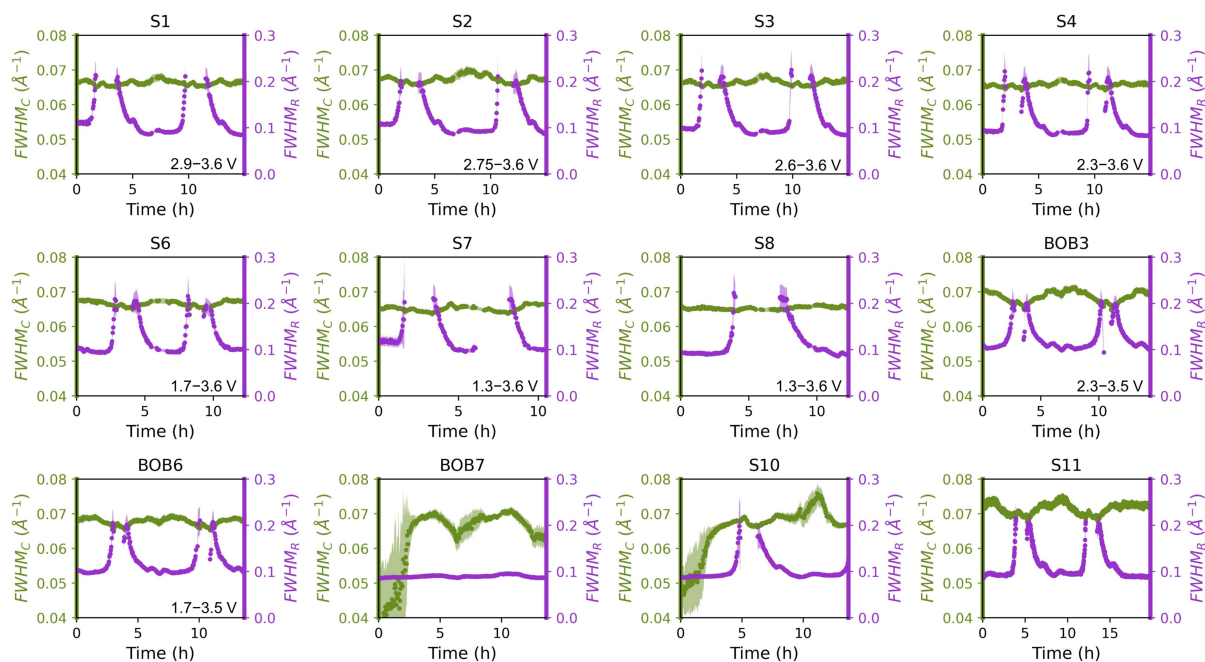


Figure S7. Refined full width at half maximum for the $Fm\bar{3}m$ and $R\bar{3}$ phases for all cells.

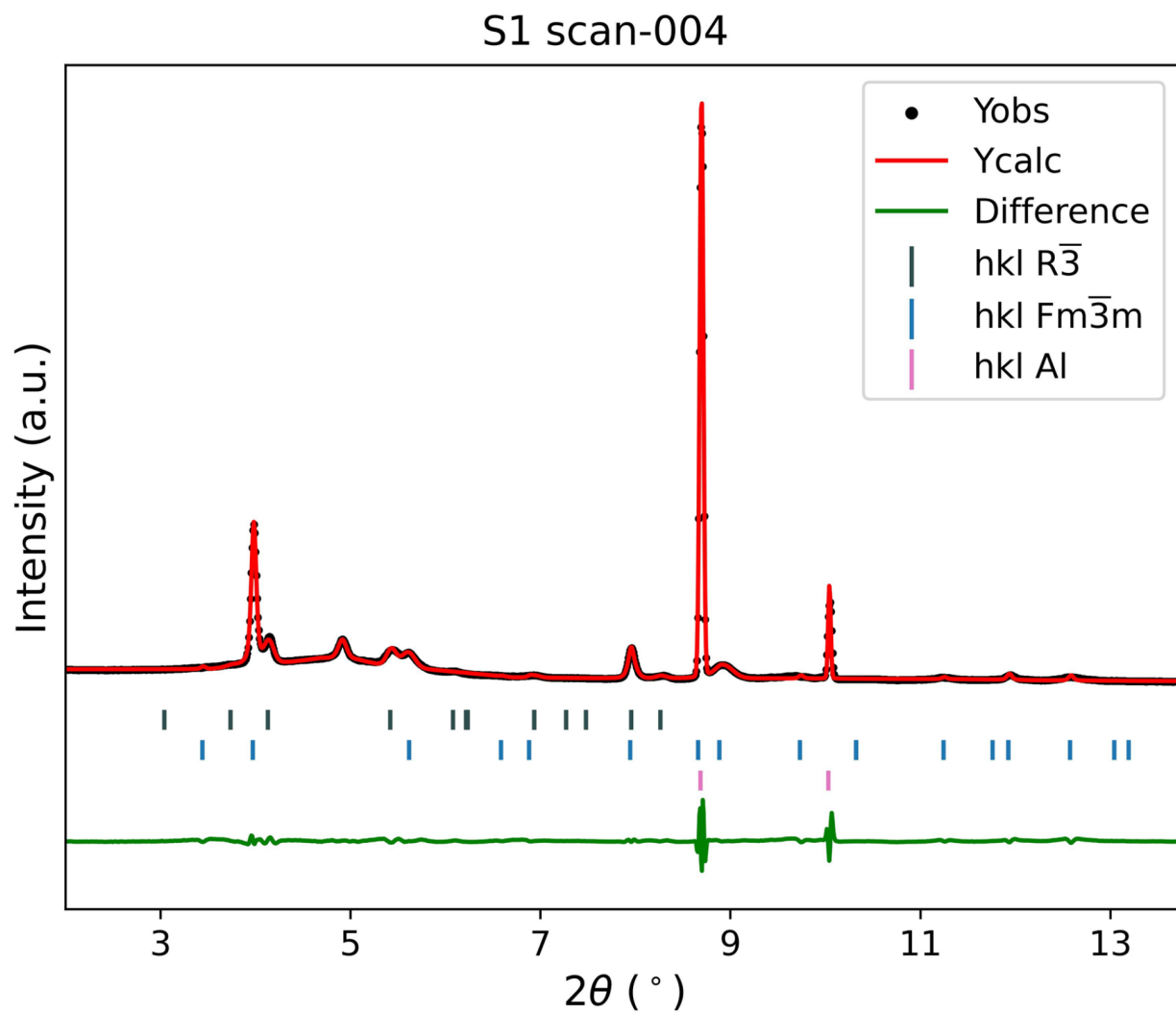


Figure S8. Representative Pawley fit of the SXRD data for cell S1 scan-0004. The peaks at 4.9, 5.6, and $8.9^\circ 2\theta$ are peaks attributed or partly attributed to the separator used in the pouch cell.

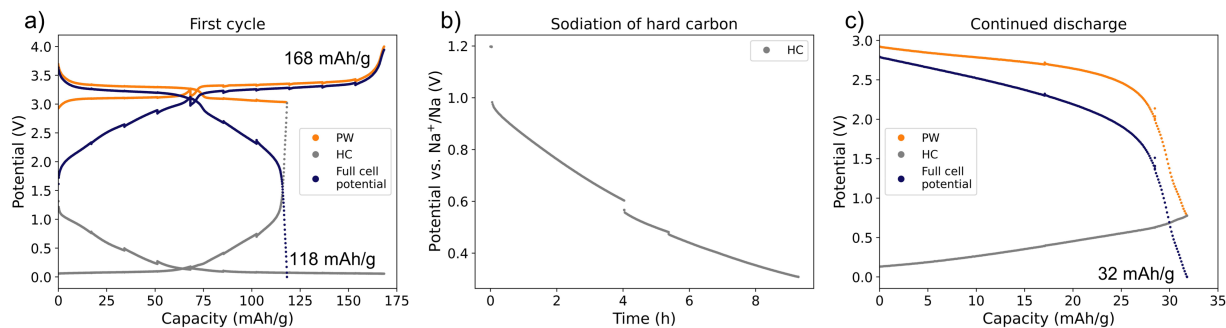


Figure S9. a) Electrochemical cycling of the 3-electrode cell consisting of PW, hard carbon, and a Na metal reference electrode (NaPF₆ in EC:DEC 1:1 v/v). b) Sodiation of the hard carbon using the Na metal reference. c) Continued discharge of the 3-electrode cell after sodiation of the hard carbon.

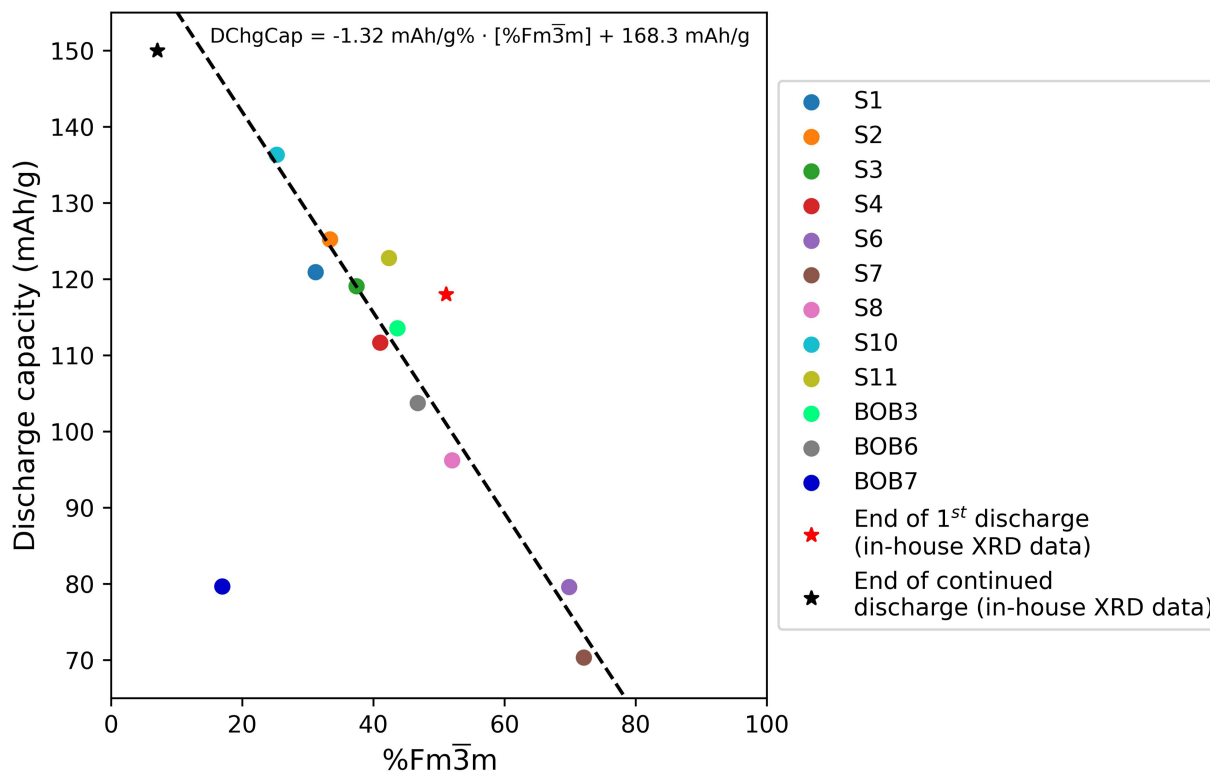


Figure S10. The discharge capacity after the first discharge at the beamtime as a function of the phase fraction updated with the results from the in-house *operando* XRD experiment.